

1 **Characterizing Continental US Hurricane Risk: Which Intensity Metric is**  
2 **Best?**

3  
4  
5 **Philip J. Klotzbach<sup>1</sup>, Daniel R. Chavas<sup>2</sup>, Michael M. Bell<sup>1</sup>, Steven G. Bowen<sup>3</sup>, Ethan J.**  
6 **Gibney<sup>4</sup>, and Carl J. Schreck III<sup>5</sup>**

7 <sup>1</sup>Department of Atmospheric Science, Colorado State University, Fort Collins, CO, USA.

8 <sup>2</sup>Department of Earth, Atmospheric and Planetary Sciences, Purdue University, West Lafayette,  
9 IN, USA.

10 <sup>3</sup>Aon, Chicago, IL, USA.

11 <sup>4</sup>Cooperative Programs for the Advancement of Earth System Science, UCAR, San Diego, CA,  
12 USA.

13 <sup>5</sup>Cooperative Institute for Satellite Earth System Studies (CISESS), North Carolina State  
14 University, Asheville, NC, USA.

15  
16 Corresponding author: Philip Klotzbach ([philk@atmos.colostate.edu](mailto:philk@atmos.colostate.edu))

17 **Key Points:**

- 18     • Minimum sea level pressure better predicts continental US hurricane damage than  
19     maximum winds or integrated kinetic energy.
- 20     • Maximum winds have historically been a poor predictor of damage caused by hurricanes  
21     making landfall from Georgia to Maine.
- 22     • Minimum sea level pressure is intrinsically an integrated wind field metric and is easy to  
23     measure, ideal for categorizing hurricane risk.  
24

**25 Abstract**

26 The damage potential of a hurricane is widely considered to depend more strongly on an  
27 integrated measure of the hurricane wind field, such as Integrated Kinetic Energy (IKE), than a  
28 point-based wind measure, such as maximum sustained wind speed ( $V_{\max}$ ). Recent work has  
29 demonstrated that minimum sea level pressure (MSLP) is also an integrated measure of the wind  
30 field. This study investigates how well historical continental US hurricane damage is predicted  
31 by MSLP compared to both  $V_{\max}$  and IKE for continental United States hurricane landfalls for  
32 the period 1988–2020. We first show for the entire North Atlantic basin that MSLP is much  
33 better correlated with IKE ( $r_{rank} = 0.50$ ) than  $V_{\max}$  ( $r_{rank} = 0.26$ ). We then show that continental  
34 US hurricane normalized damage is better predicted by MSLP ( $r_{rank} = 0.81$ ) than either  $V_{\max}$   
35 ( $r_{rank} = 0.65$ ) or IKE ( $r_{rank} = 0.68$ ). For Georgia to Maine hurricane landfalls specifically, MSLP  
36 and IKE show similar levels of skill at predicting damage, whereas  $V_{\max}$  provides effectively no  
37 predictive power. Conclusions for IKE extend to power dissipation as well, as the two quantities  
38 are highly correlated because wind radii closely follow a Modified Rankine vortex. The physical  
39 relationship of MSLP to IKE and power dissipation is discussed. In addition to better  
40 representing damage, MSLP is also much easier to measure via aircraft or surface observations  
41 than either  $V_{\max}$  or IKE, and it is already routinely estimated operationally. We conclude that  
42 MSLP is an ideal metric for characterizing hurricane damage risk.

43

**44 Plain Language Summary**

45

46 For decades, maximum sustained winds have been used to categorize potential hurricane  
47 impacts. Recent work argues that an integrated hurricane wind field measure better represents  
48 risk. Here we use historical continental U.S. hurricane and economic damage data to show that  
49 minimum sea level pressure better correlates with damage than integrated kinetic energy, a  
50 measure of hurricane vortex size and strength, or maximum sustained wind. Maximum sustained  
51 wind has been a poor damage predictor for Georgia to Maine landfalling hurricanes. Since  
52 minimum central pressure is an integrated wind field measure that only requires storm center  
53 measurements, and is already routinely estimated, we propose that minimum sea level pressure  
54 replace maximum sustained wind as the primary hurricane categorization method.

55

## 56 **1 Introduction**

57 Hurricanes are one of the most damaging natural catastrophes, causing hundreds to thousands of  
58 fatalities and billions of US dollars (USD) in damage globally each year (Mendelsohn et al.,  
59 2012; Klotzbach et al., 2018; Grinsted et al., 2019). Damage from hurricanes has grown in recent  
60 years, with a primary driver being an increase in population and wealth along the coast. Given  
61 the large impacts that hurricanes cause, ideally their intensity should be categorized using  
62 metrics that best represent their potential impacts when communicating risk to the public.

63 For more than 40 years, North Atlantic (hereafter Atlantic) and eastern North Pacific hurricanes  
64 have been categorized using the Saffir–Simpson Hurricane Scale (Simpson, 1974), although the  
65 utility of this scale has been called into question during the past ~15 years. In 2010, the National  
66 Hurricane Center removed storm surge and minimum sea level pressure (MSLP) from the scale,  
67 resulting in the modified Saffir–Simpson Hurricane Wind Scale (SSHWS; Schott et al., 2012),  
68 which categorizes hurricanes purely based on maximum sustained wind ( $V_{\max}$ ).

69 Powell and Reinhold (2007) advocated for an integrated kinetic energy (IKE) metric to  
70 categorize wind potential destruction from hurricanes. Many follow-up studies have also used  
71 IKE to categorize both individual hurricanes as well as entire hurricane seasons (e.g., Maclay et  
72 al., 2008; Misra et al., 2013; Kozar et al., 2014; Buchanan et al., 2018). Unlike  $V_{\max}$ , which  
73 simply represents a point-based estimate of the maximum sustained winds in a hurricane, IKE  
74 assesses the strength of the overall hurricane circulation. For a given  $V_{\max}$ , larger storms  
75 typically have increased storm surge (Irish et al., 2008) and larger wind and rainfall footprints  
76 (Lonfat et al., 2007).

77 Chavas et al. (2017) demonstrated that MSLP also intrinsically represents an integrated measure  
78 of the wind field that captures the combined effect of  $V_{\max}$  and storm size. Specifically, the  
79 relationship between the hurricane’s central pressure deficit (e.g., the difference in pressure  
80 between the center of the hurricane and the surrounding environment) and  $V_{\max}$  can be  
81 understood through gradient wind balance. The central pressure deficit increases predominantly  
82 with increasing  $V_{\max}$  (the canonical “wind–pressure relationship”; Knaff and Zehr (2007))  
83 but also with increasing storm size as well as background rotation rate. Hence, MSLP ought to be  
84 more similar to an IKE-type metric than  $V_{\max}$ .

85 Klotzbach et al. (2020) showed that MSLP had a statistically significant improvement in  
86 correlation with normalized continental US (CONUS) landfalling hurricane damage (Weinkle et  
87 al., 2018) relative to  $V_{\max}$  from 1900–2018 as well as direct fatalities from 1988–2018. In  
88 addition to CONUS landfalling hurricane damage, they also found a stronger relationship  
89 between MSLP and a hurricane’s average 34-kt wind radii at landfall, providing additional  
90 verification of Chavas et al. (2017)’s study and further evidence that MSLP may be more similar  
91 to IKE than  $V_{\max}$ . To date, though, a full comparison of the utility of MSLP,  $V_{\max}$ , and IKE at  
92 predicting historical damage has yet to be undertaken.

93 The purpose of this manuscript is to examine how well MSLP predicts historical damage as  
94 compared to  $V_{\max}$  and IKE for CONUS landfalling hurricanes. We first compare the three  
95 metrics for all Atlantic hurricanes, then likely well-monitored hurricanes in the southwestern  
96 portion of the basin and then lastly for CONUS landfalling hurricanes. We then compare how  
97 well each quantity predicts historical damage both overall and for Texas to Florida vs. Georgia to

98 Maine events. We also discuss the physical relationship between  $V_{\max}$ , MSLP, IKE and power  
 99 dissipation (PD; Bister & Emanuel, 1998; Emanuel, 1999).

## 100 **2 Data and Methodology**

101 The primary dataset for the analysis that follows is the Extended Best Track (Demuth et al.,  
 102 2006) that consists of intensity, location and various wind radii measurements. The location and  
 103 intensity information in the extended best track are the same as in HURDAT2 (Landsea &  
 104 Franklin, 2013) - NOAA's official Atlantic hurricane database. The Extended Best Track also  
 105 provides 34-kt, 50-kt, and 64-kt wind radii as well as the radius of maximum winds at 6-hourly  
 106 temporal resolution since 1988. Wind radii from 1988–2003 in the Extended Best Track are from  
 107 operational estimates, while the National Hurricane Center has best-tracked wind radii since  
 108 2004. Here we investigate the relationship between MSLP,  $V_{\max}$  and IKE in both the Extended  
 109 Best Track for all Atlantic hurricanes, hurricanes in the southwest Atlantic that were likely well  
 110 measured, as well as CONUS landfalling hurricanes specifically, from 1988–2020.

111 The southwest Atlantic hurricane dataset is classified using the following criteria from Chavas  
 112 and Knaff (2022):

- 113 1) Take only hurricanes from 2004 onwards, as wind radii have been best tracked by the  
 114 National Hurricane Center since that time
- 115 2) Select only hurricane positions where the center was located at or south of 30°N, to reduce  
 116 any signal from extratropical transition
- 117 3) Take only hurricanes where the center was located at or west of 50°W, since these storms are  
 118 more likely to have been observed by aircraft reconnaissance
- 119 4) Remove any hurricane locations whose distance to land is less than its mean  $R_{34kt}$  value, to  
 120 reduce potential land interaction impacts on wind radii

121 Continental US landfalling hurricane MSLP and  $V_{\max}$  are taken from the Atlantic Oceanographic  
 122 and Meteorological Laboratory website:

123 [https://www.aoml.noaa.gov/hrd/hurdat/UShurrs\\_detailed.html](https://www.aoml.noaa.gov/hrd/hurdat/UShurrs_detailed.html) that is based on HURDAT2. As  
 124 was done in Klotzbach et al. (2020), we do count Sandy (2012) as a hurricane landfall, since it  
 125 brought severe damage to the mid-Atlantic states and was a hurricane until just a few hours  
 126 before landfall when it became extratropical.

127 Normalized damage estimates, that is, the amount of damage a hurricane would likely cause if it  
 128 were to make landfall today given inflation and changes in exposure, are taken from Weinkle et  
 129 al. (2018) for hurricane landfalls from 1988–2017, while damage estimates for the ten CONUS  
 130 landfalling hurricanes from 2018–2020 are taken from the National Hurricane Center best track  
 131 reports on these storms (<https://www.nhc.noaa.gov/data/tcr/>). Normalized damage estimates from  
 132 Weinkle et al. (2018) are provided in 2018 USD, while damage estimates from the hurricane  
 133 landfalls of 2018–2020 are listed in USD of the year that they made landfall. Changes in  
 134 inflation, population and exposure should be relatively minor factors from 2018–2020.

135 Multiple landfalls from the same hurricane are identified if there were two separate damage  
 136 estimates recorded in the Weinkle et al. (2018) dataset. From 1988–2017, three hurricanes were  
 137 recorded with two separate damage estimates: Andrew (1992), Erin (1995), and Georges (1998).  
 138 The results would not change significantly if only one landfall per storm were considered. None  
 139 of the ten CONUS landfalling hurricanes in 2018–2020 made multiple landfalls, defined in  
 140 Klotzbach et al. (2018) and here to be two separate CONUS hurricane landfalls with at least 100  
 141 miles of open ocean between landfalls.

142 Integrated kinetic energy is defined as:

$$143 \quad IKE = \int_0^{2\pi} \int_0^{r_0} \frac{1}{2} \rho h V^2 r dr d\theta \quad (1)$$

144 where  $r$  is radius,  $V$  is total wind speed,  $\rho$  is near-surface air density, and  $h$  is a fluid depth. The  
 145 latter two may be assumed constant and so are not important for our analysis. We estimate IKE  
 146 following the methodology of Misra et al. (2013), which sets  $\rho=1 \text{ kg m}^{-3}$  and  $h=1 \text{ m}$  and then  
 147 uses the estimates of the radius of maximum wind ( $R_{\max}$ ) and the four quadrant estimates of the  
 148 radius of 34-kt wind ( $R_{34\text{kt}}$ ), radius of 50-kt wind ( $R_{50\text{kt}}$ ) and radius of 64-kt wind ( $R_{64\text{kt}}$ ) from  
 149 the Extended Best Track. The method calculates the area within each quadrant between each pair  
 150 of adjacent wind radii and uses a representative wind speed between the bounding wind speeds.  
 151 IKE is then summed across all quadrant sub-regions. The algorithm is summarized in Table S1,  
 152 which is identical to Table A1 of Misra et al. (2013), with one minor modification to clarify the  
 153 criteria within the hurricane-force wind region (Misra personal communication. 2021–06–23).  
 154 Approximately 1% of 6-hourly periods in the extended best track are excluded (all prior to 2003)  
 155 either due to lack of radius of maximum winds or 34-kt wind radii which is necessary to  
 156 calculate IKE.

157 Integrated kinetic energy at landfall was calculated as the IKE at the six-hourly period between  
 158 12–18 hours prior to landfall, since the wind radii necessary to calculate IKE are only given  
 159 at six-hourly intervals recorded in the best track (e.g., 0, 6, 12, 18 UTC). Integrated kinetic  
 160 energy at this time period had slightly higher correlations with  $V_{\max}$ , MSLP and normalized  
 161 damage than adjacent six-hour periods. As a hurricane gets closer to landfall, the outer  
 162 circulation of the storm is already on land, likely causing deformation of the hurricane wind  
 163 field. If different time periods were used to calculate landfalling IKE, the results would only  
 164 change slightly.

165 We also compare results using IKE to those using power dissipation (PD; Bister & Emanuel,  
 166 1998). Power dissipation scales identically with IKE except with the wind speed cubed rather  
 167 than squared, and is given by:

$$168 \quad PD = \int_0^{2\pi} \int_0^{r_0} \rho C_d V^3 r dr d\theta \quad (2)$$

169  
 170 where  $\rho$  is near-surface air density and  $C_d$  is the surface drag coefficient, each of which may be  
 171 taken as approximately constant and so are not important for our analysis. Here we set  $\rho =$   
 172  $1 \text{ kg/m}^3$  and  $C_d = 10^{-3}$ . We calculate PD following the same methodology as IKE above, but  
 173 cubing rather than squaring the wind speed.  
 174

175 Rank correlations ( $r_{rank}$ ) are used as the predominant agreement metric between time series  
 176 throughout the manuscript, in order to remove the influence of large outlying events (e.g.,  
 177 Katrina for normalized damage or Sandy for IKE). Higher ranks are defined to be higher  $V_{max}$ ,  
 178 lower MSLP (e.g., deeper storms), higher IKE and increased damage. We find that MSLP is a  
 179 consistently better predictor of historical damage than both  $V_{max}$  and IKE, and we discuss the  
 180 implications of this result given that MSLP is inherently an integrated measure of the wind field  
 181 whose estimation is straightforward and already routinely measured.

182 Statistical significance is primarily calculated using bootstrap resampling methods and is  
 183 reported at the 5% level (Efron, 1979; Hesterberg et al., 2003). Statistical significance of  
 184 correlations are calculated by resampling with replacement 1000 times from the dataset being  
 185 investigated. If fewer than 5% of the randomly resampled correlations are less than zero, the  
 186 correlation is said to be significant. Statistical significance of correlation differences is calculated  
 187 using the Fisher  $r$  to  $z$  transformation and accounting for the correlation between the two time  
 188 series (Lee & Preacher, 2013).

### 189 **3 Relationships between $V_{max}$ , MSLP and IKE**

#### 190 **3.1 Full Atlantic basin**

191 We begin by investigating the relationship between MSLP,  $V_{max}$ , and IKE for all Atlantic  
 192 hurricanes from 1988–2020 and find that IKE covaries strongly with MSLP but not  
 193  $V_{max}$ . Overall, for all Atlantic hurricanes, the correlation between MSLP and IKE is significantly  
 194 stronger ( $r_{rank} = 0.50$ ) than between  $V_{max}$  and IKE ( $r_{rank} = 0.26$ ).

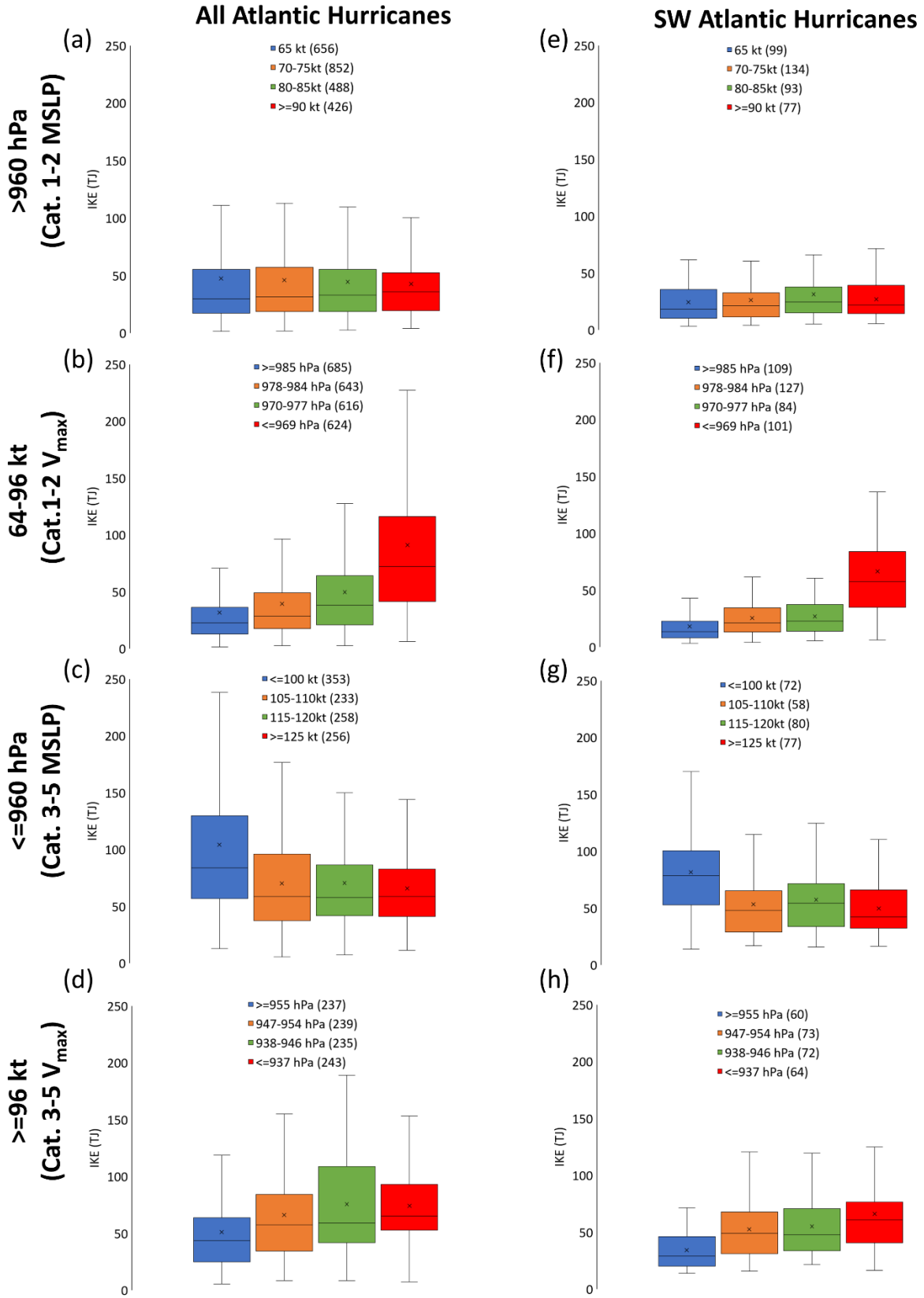
195 We visualize this closer relationship between MSLP and IKE for both Category 1–2 hurricanes  
 196 and major (Category 3–5) hurricanes in Figure 1. Figure 1a displays a boxplot of IKE for the  
 197 approximate quartiles of  $V_{max}$  for Atlantic hurricanes<sup>1</sup> classified as Category 1–2 based on  
 198 MSLP, using the Klotzbach et al. (2020) definition (e.g., >960 hPa). There is no systematic  
 199 variation in IKE across quartiles of  $V_{max}$  (Figure 1a), indicating that  $V_{max}$  provides little  
 200 additional information about IKE beyond what is provided by MSLP.

201 In contrast, if we take Category 1–2 hurricanes by  $V_{max}$  (e.g., 64–95 kt) and plot quartiles of  
 202 MSLP (Figure 1b), there is a pronounced trend towards larger IKE values at higher pressure  
 203 intensity (i.e., lower MSLP). For example, mean IKE for the strongest quartile of MSLP ( $\leq 969$   
 204 hPa) is three times larger than for the weakest quartile of MSLP ( $\geq 986$  hPa).

205 Results are similar for major hurricanes defined by MSLP ( $\leq 960$  hPa) and  $V_{max}$  ( $\geq 96$  kt).  $V_{max}$   
 206 generally shows a weak relationship with IKE (Figure 1c), whereas lower MSLP generally is  
 207 associated with larger values of IKE (Figure 1d).

---

<sup>1</sup>Atlantic hurricanes are classified in 5 kt increments, which precludes a more precise stratification by quartiles. For example, 27% of all 6-hr periods for Category 1–2 hurricanes classified by MSLP are 65 kt, 18% are 70 kt, 17% are 75 kt, 11% are 80 kt, 8% are 85 kt, while hurricanes with  $V_{max} \geq 90$  kt comprise the remaining 19% of the sample. The closest to a quartile breakdown that we can make is: 65 kt (27%), 70–75 kt (35%), 80–85 kt (19%) and  $\geq 90$  kt (19%)



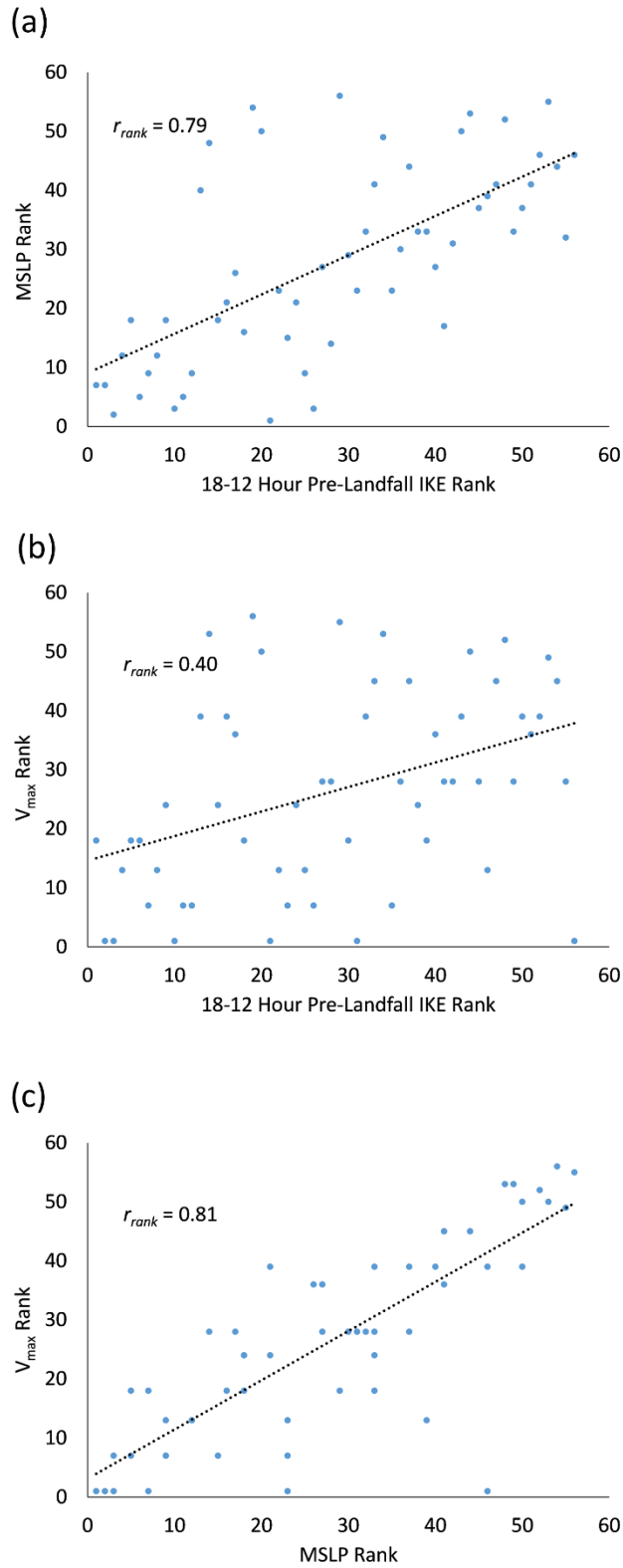
209 **Figure 1.** Quartile box plots showing relationships between MSLP,  $V_{\max}$ , and IKE for Atlantic  
210 hurricanes. (a) Box plot of IKE for approximate quartiles of  $V_{\max}$  for all Atlantic Category 1–2  
211 hurricanes as classified by MSLP from 1988–2020. Numbers in parentheses represent the  
212 number of six-hourly hurricane observations in each quartile. (b) As in panel a but for Category  
213 1–2 hurricanes classified by  $V_{\max}$ . (c) As in panel a but for all Atlantic major hurricanes  
214 classified by MSLP from 1988–2020. (d) As in panel a but for all Atlantic major hurricanes  
215 classified by  $V_{\max}$  from 1988–2020. (e–h) As in panels a–d but for southwest Atlantic hurricanes  
216 from 2004–2020. The middle line in all box plots represents the median value, while the ‘x’ in  
217 all box plots represents the mean value.

### 218 **3.2 Southwest Atlantic hurricanes**

219 Our results are similar when focusing on the subset of cases from the Extended Best Track  
220 dataset from the southwest Atlantic Ocean since 2004 that are expected to be well-sampled by  
221 aircraft (Figures 1e–h). The correlation between MSLP and IKE in the subset of the best sampled  
222 cases is stronger ( $r_{\text{rank}} = 0.63$ ) than it was for the entire Atlantic basin over the longer record, and  
223 it remains significantly stronger than between  $V_{\max}$  and IKE ( $r_{\text{rank}} = 0.45$ ). For Category 1–2  
224 hurricanes, IKE again shows little systematic variation with  $V_{\max}$  (Figures 1e and 1g), while  
225 systematically increasing with decreasing MSLP (Figures 1f and 1h).

### 226 **3.3 Continental United States landfalling hurricanes**

227 We next show that these relationships extend specifically to CONUS landfalling hurricanes at  
228 landfall. Figures 2a–2c display scatterplots of the relationship between MSLP and IKE,  $V_{\max}$  and  
229 IKE, and  $V_{\max}$  and MSLP, respectively, for CONUS landfalling hurricanes. As was the case for  
230 basinwide hurricanes, there is a significantly stronger relationship between MSLP and IKE ( $r_{\text{rank}}$   
231  $= 0.79$ ) than between  $V_{\max}$  and IKE ( $r_{\text{rank}} = 0.40$ ) for CONUS landfalling hurricanes.



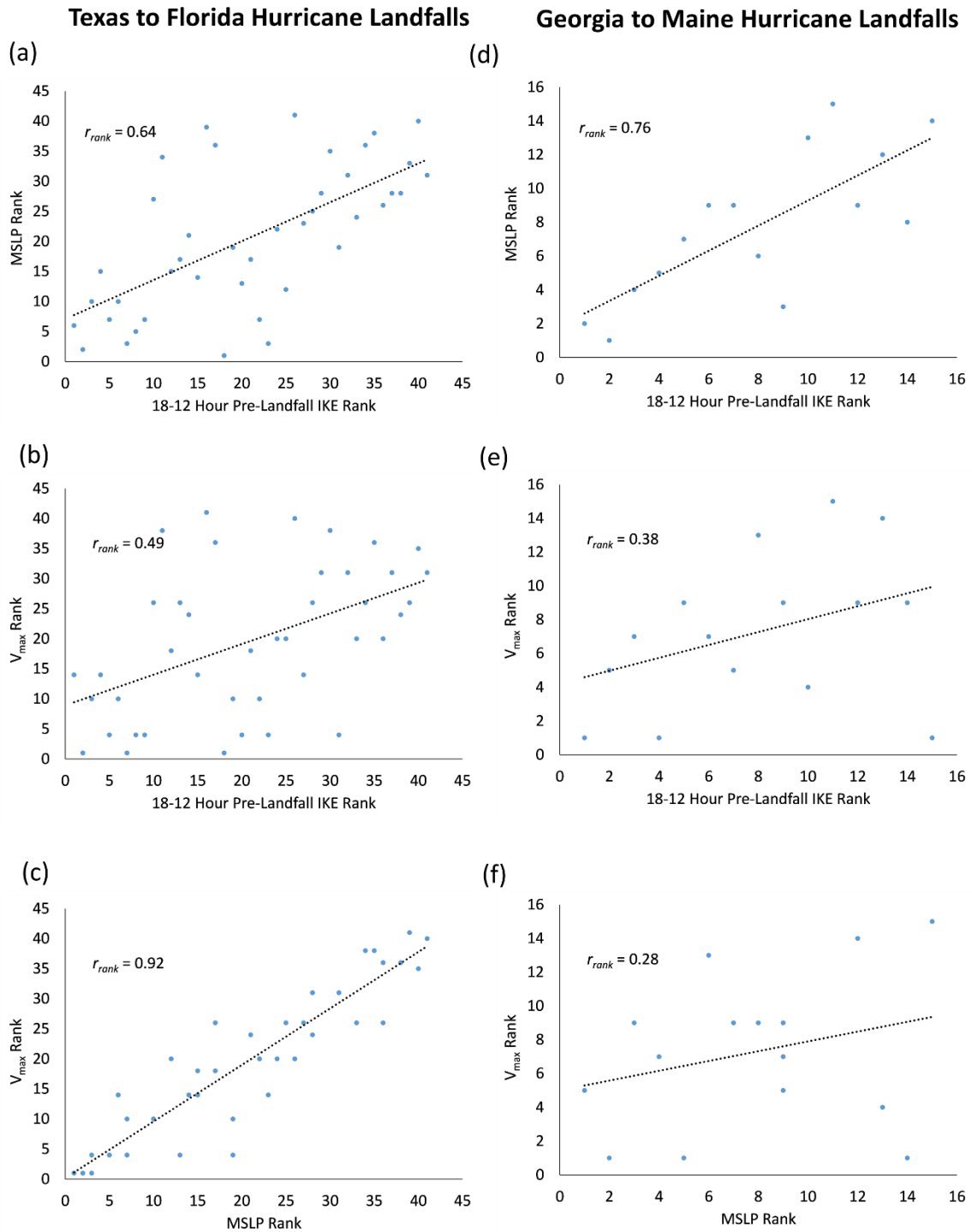
232

233 **Figure 2.** Relationship between MSLP,  $V_{max}$  and IKE for CONUS landfalling hurricanes from  
 234 1988–2020. (a) Rank scatterplot of MSLP and IKE for CONUS landfalling hurricanes. (b) As in  
 235 panel a but for  $V_{max}$  and IKE. (c) As in panel a but for  $V_{max}$  and MSLP.

**236 3.4 Texas to Florida vs. Georgia to Maine landfalling hurricanes**

237 Results are similar when we decompose landfalls by region for Texas to Florida landfalls and  
238 Georgia to Maine landfalls. For Texas to Florida landfalls (Figures 3a–3c) the correlation  
239 between MSLP and IKE ( $r_{\text{rank}} = 0.64$ ) is greater than the correlation between  $V_{\text{max}}$  and IKE ( $r_{\text{rank}}$   
240  $= 0.49$ ). For Georgia to Maine landfalls (Figures 3d–3f) the correlation between MSLP and IKE  
241 ( $r_{\text{rank}} = 0.76$ ) is again greater than the correlation between  $V_{\text{max}}$  and IKE ( $r_{\text{rank}} = 0.38$ ), which is a  
242 starker contrast between MSLP and  $V_{\text{max}}$  than for Texas to Florida landfalls. While the  
243 relationship between  $V_{\text{max}}$  and MSLP is significant and strong for Texas to Florida landfalls  
244 ( $r_{\text{rank}} = 0.92$ ), the correlation is weak and insignificant for Georgia to Maine landfalls ( $r_{\text{rank}} =$   
245  $0.28$ ). Hurricanes tend to grow in size as they move poleward (Knaff et al. 2014, Chavas et al.  
246 2016, Klotzbach et al. 2020, Chavas and Knaff 2022), and have a larger radius of maximum  
247 wind as a result (Chavas and Knaff 2022), which increases variations in IKE that may be  
248 captured by MSLP but not  $V_{\text{max}}$ .

249



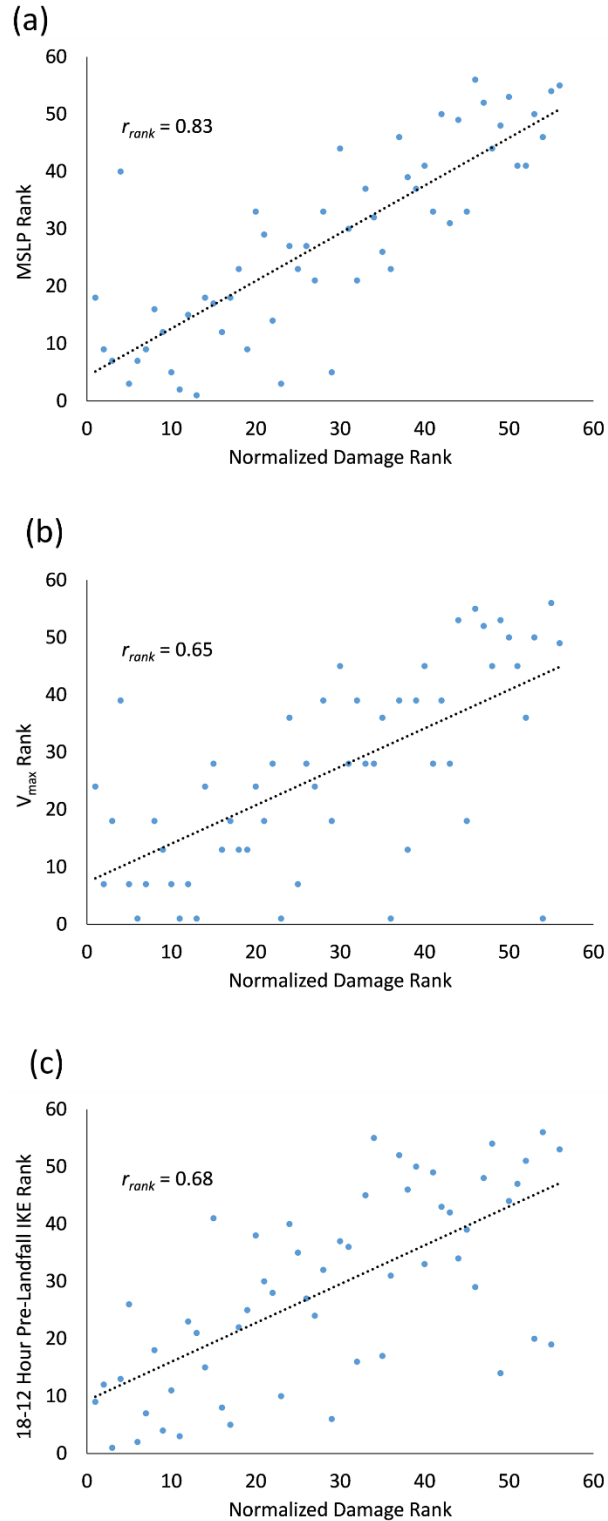
250

251 **Figure 3.** Relationship between MSLP,  $V_{max}$  and IKE for Texas to Florida landfalling hurricanes  
 252 (left column) and Georgia to Maine landfalling hurricanes (right column) from 1988–2020. (a)  
 253 Rank scatterplot of MSLP and IKE for Texas to Florida landfalling hurricanes. (b) As in panel a  
 254 but for  $V_{max}$  and IKE. (c) As in panel a but for  $V_{max}$  and MSLP. (d–f) As in a–c but for Georgia  
 255 to Maine landfalling hurricanes.

## 256 **4 Relationship between intensity metrics and normalized landfalling hurricane damage**

### 257 **4.1 Continental United States normalized landfalling hurricane damage**

258 We now show that MSLP better predicts historical damage as compared to IKE or  $V_{\max}$ ,  
259 beginning with the entire US coastline. Figures 4a–c display relationships between MSLP,  $V_{\max}$   
260 and IKE with CONUS normalized damage, with higher ranks indicating stronger storms and  
261 increased damage. The correlation between MSLP and CONUS normalized damage ( $r_{\text{rank}} =$   
262 0.83; Figure 4a) is significantly stronger (as highlighted by the stronger slope of the best fit line)  
263 than the correlation between  $V_{\max}$  and CONUS normalized damage ( $r_{\text{rank}} = 0.65$ ; Figure 4b). The  
264 MSLP-CONUS normalized damage correlation is also significantly stronger than the correlation  
265 between IKE and CONUS normalized damage ( $r_{\text{rank}} = 0.68$ ; Figure 4c).



266

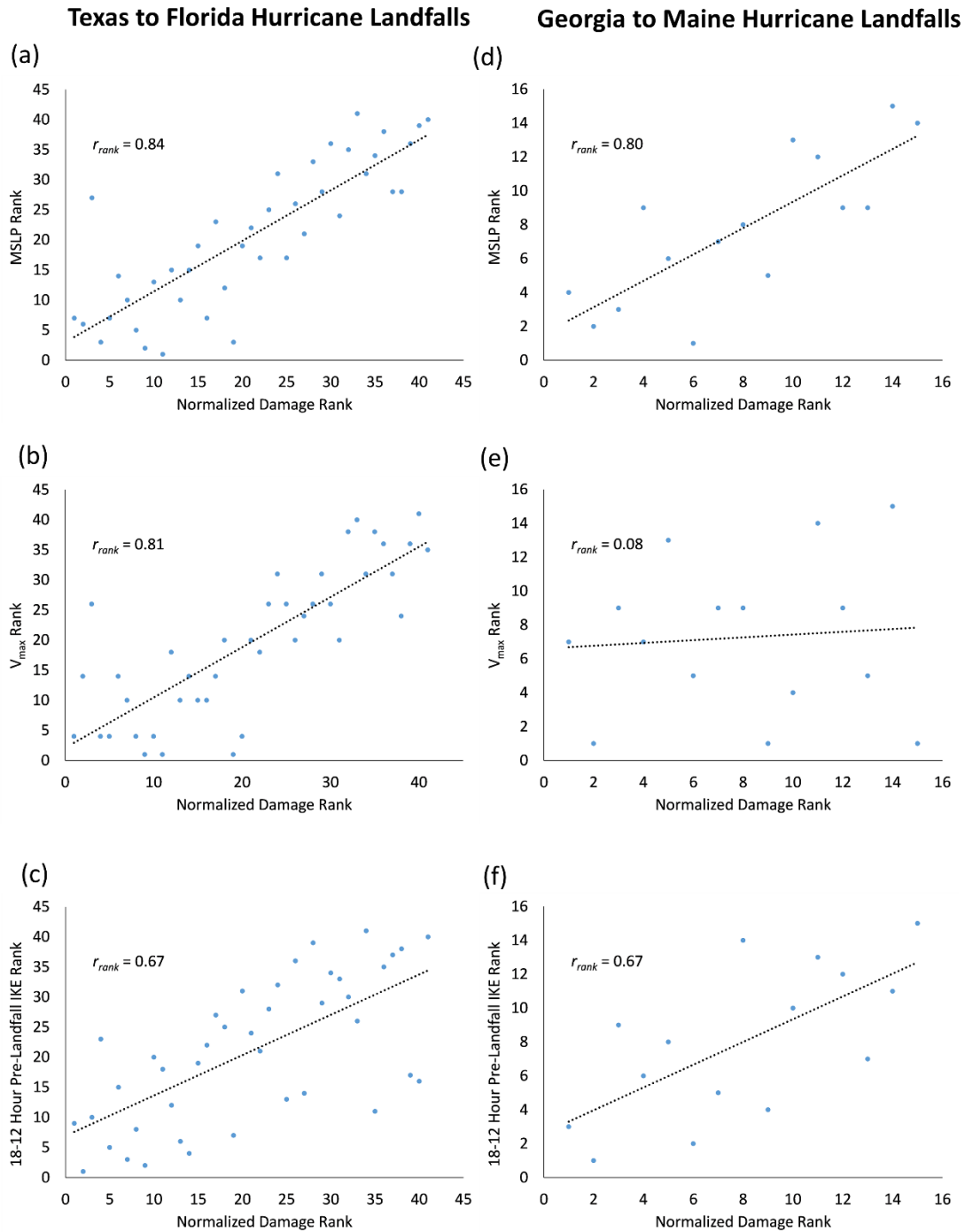
267 **Figure 4.** Relationship between intensity metrics and CONUS landfalling hurricane damage  
268 from 1988–2020. (a) Rank scatterplot of MSLP and damage from CONUS landfalling  
269 hurricanes. (b) As in panel a but for  $V_{max}$  and damage from CONUS landfalling hurricanes. (c)  
270 As in panel a but for IKE and damage from CONUS landfalling hurricanes.

**271 4.2 Texas to Florida vs. Georgia to Maine normalized landfalling hurricane damage**

272 Klotzbach et al. (2020) noted similar correlations for Texas to Florida hurricane landfalls  
273 between  $V_{\max}$  and normalized damage as between MSLP and normalized damage, while MSLP  
274 was a much more skillful predictor of damage than  $V_{\max}$  for Georgia to Maine hurricane  
275 landfalls. We now show that MSLP is also a better predictor for these two regions compared to  
276 both IKE and  $V_{\max}$ , particularly for Georgia to Maine.

277 For Texas to Florida landfalls, the correlation between MSLP and normalized damage ( $r_{\text{rank}} =$   
278  $0.84$ ; Figure 5a) and  $V_{\max}$  and normalized damage ( $r_{\text{rank}} = 0.81$ ; Figure 5b) are both strong and  
279 nearly equal. Meanwhile, the correlation between IKE and normalized damage is slightly weaker  
280 ( $r_{\text{rank}} = 0.67$ ; Figure 5c). These results for the relationship between both  $V_{\max}$  and MSLP with  
281 normalized damage are similar to that of Klotzbach et al. (2020).

282 For Georgia to Maine landfalls, the correlation between MSLP and normalized damage is strong  
283 ( $r_{\text{rank}} = 0.80$ , Figure 5d). The correlation between IKE and normalized damage is a bit weaker  
284 ( $r_{\text{rank}} = 0.67$ , Figure 5f). Both of these correlations are similar to their Texas to Florida  
285 correlation values. However, the correlation between  $V_{\max}$  and normalized damage is extremely  
286 weak ( $r_{\text{rank}} = 0.08$ , Figure 5e) and is not significant. Hence, hurricane metrics that either  
287 explicitly (IKE) or implicitly (MSLP) have a size component are more skillful for hurricanes  
288 making landfall along the East Coast of the United States north of Florida. This result for  
289 damage aligns with the finding above that  $V_{\max}$  itself is poorly correlated with IKE for this  
290 landfall region ( $r_{\text{rank}} = 0.38$ , Figure 3e).



291

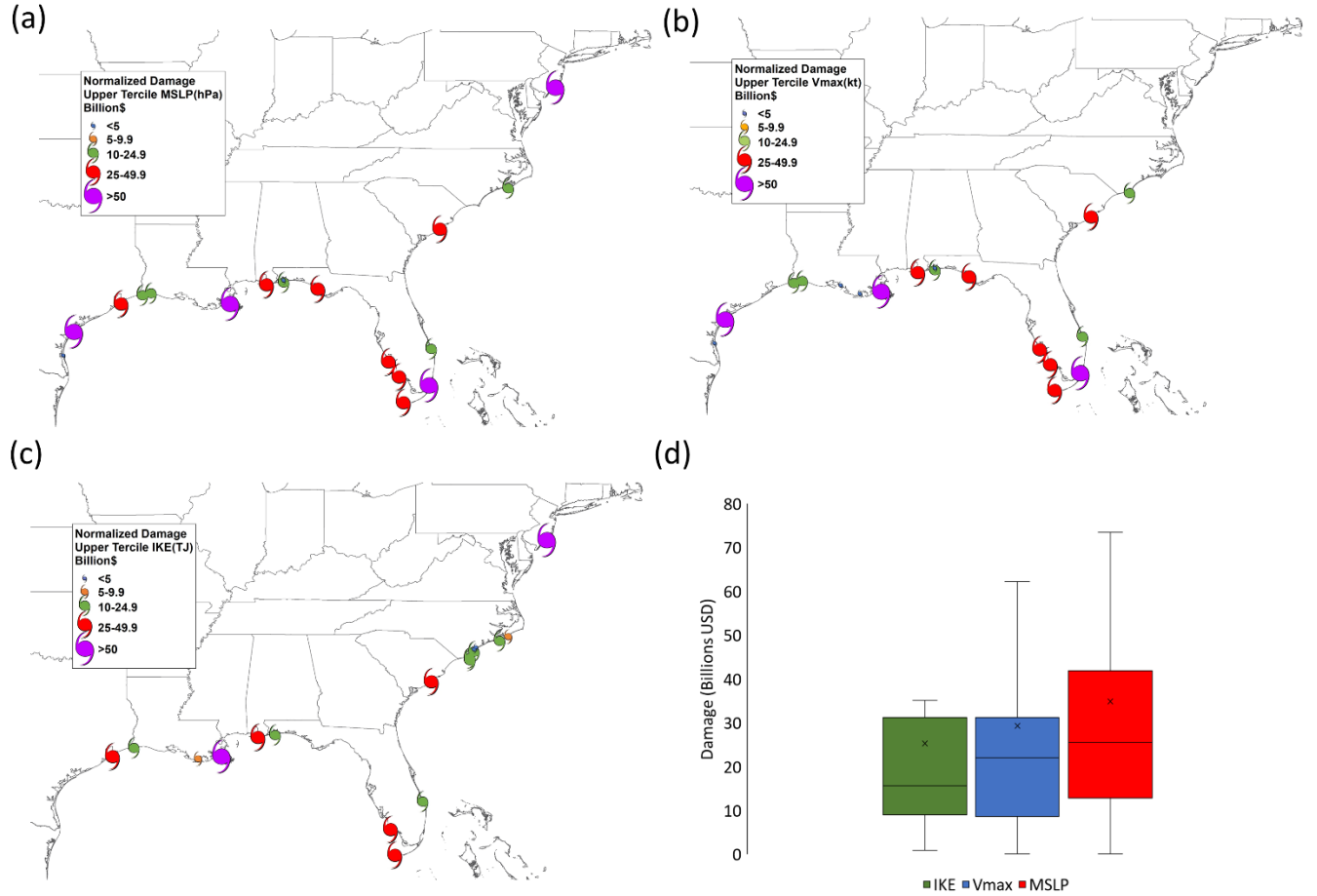
292 **Figure 5.** Relationship between MSLP,  $V_{\max}$  and IKE with normalized damage for Texas to  
 293 Florida landfalling hurricanes (left column) and Georgia to Maine landfalling hurricanes (right  
 294 column) from 1988–2020. (a) Rank scatterplot of MSLP and normalized damage for Texas to  
 295 Florida landfalling hurricanes. (b) As in panel a but for  $V_{\max}$  and normalized damage for Texas  
 296 to Florida landfalling hurricanes. (c) As in panel a but for IKE and normalized damage for Texas  
 297 to Florida landfalling hurricanes. (d–f) As in a–c but for Georgia to Maine landfalling hurricanes.

298 A prime example of this is Sandy (2012), whose  $V_{\max}$  was barely at hurricane-equivalent  
299 intensity at landfall yet had a very low MSLP owing in part to its exceptionally large size  
300 (Halverson & Rabenhorst 2013; Chavas et al. 2018). We note that the correlation between  $V_{\max}$   
301 and normalized damage for Georgia to Maine is considerably lower than what was found in  
302 Klotzbach et al. (2020) from 1900–2018 ( $r_{\text{rank}} = 0.42$ ). The degradation in the correlation is due  
303 to a relatively smaller sample size of Georgia to Maine hurricane landfalls from 1988–2020 (e.g.,  
304 15 landfalls) that also includes Sandy. One outlier in a small sample can considerably impact a  
305 correlation value. If Sandy were excluded from the 1988–2020 analysis, the correlation between  
306  $V_{\max}$  and normalized damage for Georgia to Maine would remain insignificant ( $r_{\text{rank}} = 0.29$ ) but  
307 would be more in line with the correlation reported in Klotzbach et al. (2020).

#### 308 **4.3 Upper tercile of continental US landfalling hurricane damage**

309 As an alternative way of demonstrating the value of MSLP as a damage predictor, we show that  
310 the historical damage caused by the strongest storms is systematically higher when storm  
311 strength is defined by MSLP. From 1988–2020, 18 hurricanes made landfall in the CONUS with  
312 a maximum intensity of 100 kt or greater - Category 3+ on the Saffir–Simpson Hurricane Wind  
313 Scale. Given that 56 CONUS landfalling hurricanes occurred from 1988–2020, this equates to  
314 the approximate upper tercile of landfalling hurricanes during the 33-year period. Figures 6a–c  
315 display the location of the 18 strongest landfalling hurricanes using MSLP ( $\leq 952$  hPa),  $V_{\max}$   
316 ( $\geq 100$  kt) and IKE ( $\geq 71$  TJ) criteria. While the spatial distribution of the upper tercile using  
317 MSLP (Figure 6a) and  $V_{\max}$  (Figure 6b) is similar, many more hurricanes from Georgia to Maine  
318 classify as upper tercile storms using IKE (Figures 6c). Using  $V_{\max}$ , two hurricanes from Georgia  
319 to Maine are in the upper tercile (Hugo (1989) and Fran (1996)). Using MSLP, in addition to  
320 Hugo and Fran, Sandy (2012) also is in the upper tercile. Using IKE, half of the 18 hurricanes in  
321 the upper tercile made landfall from Georgia to Maine. The larger number of high-IKE landfalls  
322 from Georgia to Maine is likely due to the growth in size of hurricanes as they move poleward  
323 and the relatively strong weighting of 34-kt and 50-kt wind radii in the IKE equation (discussed  
324 in more detail in the next section).

325 Finally, Figure 6d displays a box plot for normalized damage for the upper tercile of landfalling  
326 hurricanes with intensity defined using MSLP, IKE, or  $V_{\max}$ . The mean, median and high  
327 quantiles of normalized damage are all largest when using MSLP, second largest when using  
328 IKE, and smallest when using  $V_{\max}$ . This analysis again highlights the improved relationship  
329 using MSLP than either IKE or  $V_{\max}$  for representing the damage potential from hurricanes.



330

331 **Figure 6.** Location and relationship between the upper tercile of hurricane intensity categorized  
 332 by MSLP,  $V_{\max}$ , and IKE and normalized damage. (a) Location of upper tercile CONUS  
 333 landfalling hurricanes from 1988–2020 based on MSLP with the size of the hurricane symbol  
 334 proportional to the normalized damage. (b) As in panel a but for the upper tercile based on  $V_{\max}$ .  
 335 (c) As in panel a but for the upper tercile based on IKE. (d) Box plot showing the distribution of  
 336 normalized damage for the upper tercile of CONUS landfalling hurricanes classified by IKE,  
 337  $V_{\max}$  and MSLP.

### 338 5 Physical discussion

339 As shown above, an integral measure of the storm wind field (MSLP or IKE) is preferable to a  
 340 point estimate of the maximum wind speed for predicting potential damage, with MSLP  
 341 performing best. Here we show how MSLP represents a radial integral of the wind field, and  
 342 how that integral weights wind speeds at different radii differently from IKE.

343

344 For an axisymmetric field, a radially-integrated quantity,  $X$ , may be written as:

345

346

$$X = \int_0^{r_0} x \, dr \quad (3)$$

347

348 where  $x$  is the integrand and  $r_0$  is some larger radius (e.g.,  $R_{34kt}$ ). For ease of interpretation we  
 349 may neglect multiplicative factors in each equation that may be taken as approximately constant,  
 350 as we use these quantities purely as statistical predictors of damage. Thus, absolute magnitudes  
 351 do not matter.

352

353 MSLP represents a reduction in pressure at the storm center relative to the ambient  
 354 environmental pressure  $P_{env}$  at the outer edge of the storm. This pressure difference is commonly  
 355 referred to as the central pressure deficit:

356

$$357 \quad dP = P_{env} - MSLP \quad (4)$$

358

359 and is related to the wind field via gradient wind balance (Knaff and Zehr 2007, Chavas et al  
 360 2017). Hence, for  $dP$ , the integrand is given by:

361

$$362 \quad x_{dP} \sim \frac{V^2}{r} + fV \quad (5)$$

363

364 where we drop the density factor ( $\rho$ ). For IKE, from Eq. (1) the integrand is given by:

365

$$366 \quad x_{IKE} \sim rV^2 \quad (6)$$

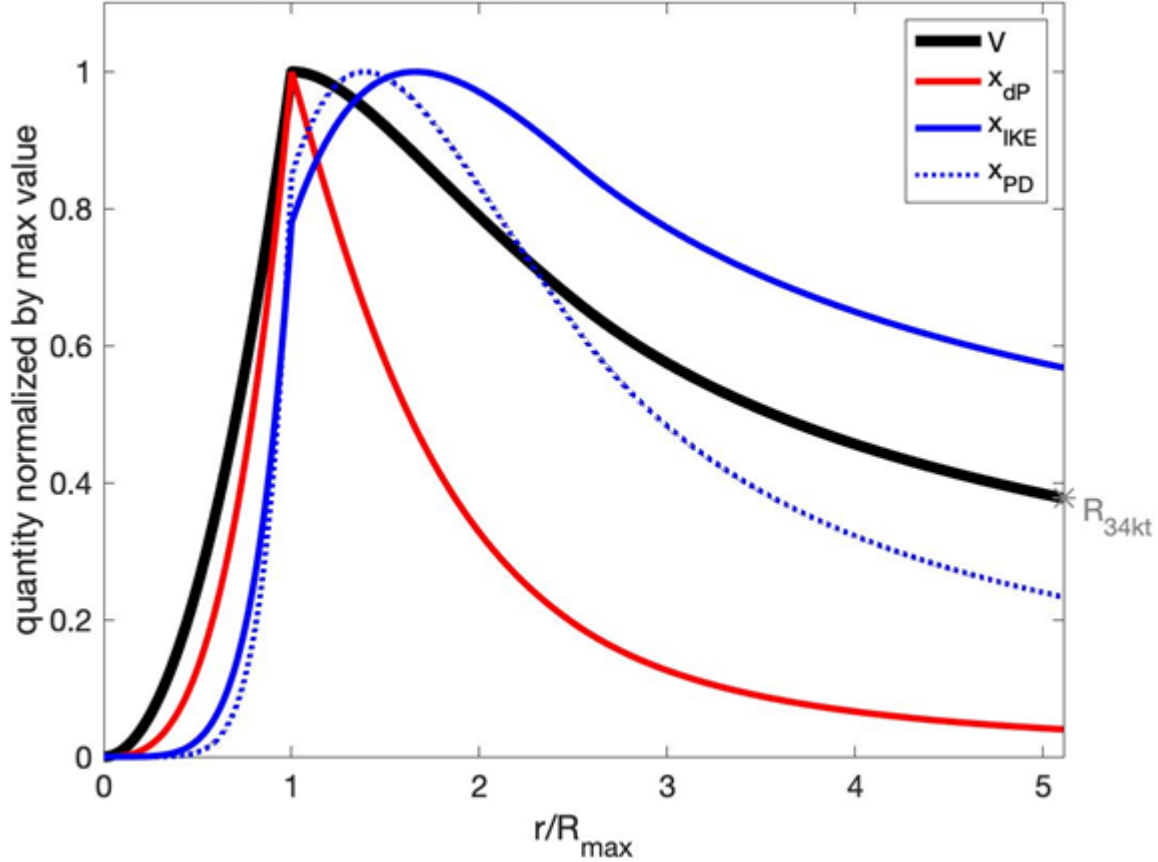
367

368 where  $r$  arises from the polar integral, and we drop the factor  $\frac{1}{2}\rho h$ .

369

370 To show how each quantity weights wind speeds at different radii, each integrand  $x$  may be  
 371 normalized by its maximum value, and the result analyzed as a function of radius normalized by  
 372 the radius of maximum wind. An example calculation is shown in Figure 7 for a characteristic  
 373 hurricane wind profile defined by the model of Chavas et al. (2015). This model has been shown  
 374 to capture the observed structure of the complete hurricane wind field as well as the basic  
 375 structural relationships between  $R_{max}$ ,  $R_{34kt}$ , and  $V_{max}$  in the historical record (Chavas and Knaff  
 376 2022). For this example, the model is defined using parameter values taken as the median values  
 377 of southwest Atlantic hurricanes:  $R_{max} = 28$  km,  $V_{max} = 90$  kt, and latitude at  $23.7^\circ N$ . The central  
 378 pressure deficit is weighted towards the strongest wind speeds in the inner core ( $r < 2R_{max}$ ),  
 379 and its maximum weighting is at  $R_{max}$  itself. Integrated kinetic energy has a similar qualitative  
 380 structure but more strongly weights weaker wind speeds at larger radii towards  $R_{34kt}$ , with its  
 381 maximum value at about  $1.7R_{max}$ . This difference arises because  $V^2$  is weighted inversely by  
 382 radius in the centrifugal term  $\frac{V^2}{r}$  in  $x_{dP}$ , and so  $x_{dP}$  decreases rapidly beyond  $R_{max}$ , whereas  $V^2$   
 383 is weighted proportionally to radius in  $x_{IKE}$ .

384



385  
386

387 **Figure 7.** Radial structure of the pressure deficit (dP; red), integrated kinetic energy (IKE; blue),  
388 and power dissipation (PD; cyan) calculated from an example tropical cyclone wind profile ( $V$ ;  
389 black). Each quantity is normalized by its maximum value, and radius is normalized by the  
390 radius of maximum wind,  $R_{\max}$ . The wind profile is defined using the physical model of Chavas  
391 et al. (2015) taking as input the median values of southwest Atlantic hurricanes:  $V_{\max} = 90$  kt,  
392  $R_{\max} = 28$  km, and latitude at  $23.7^{\circ}\text{N}$ . A simple quadratic profile is used in the eye for  $r < R_{\max}$ .  
393  $R_{34kt}$  is marked with a gray star. Each colored curve represents the integrand whose radial  
394 integral scales with the given quantity. This quantity is normalized by its maximum value to  
395 allow for direct comparison across dP, IKE, and PD (see text for details).

396

397 A viable alternative integral quantity to IKE is PD. Power dissipation scales identically with IKE  
398 except with the wind speed cubed rather than squared. While IKE (units of Joules) is much more  
399 widely used, PD (units of Watts) has physical appeal for damage potential because it represents  
400 the rate of transfer of kinetic energy from the near-surface air into the surface due to surface  
401 friction. For PD, from Eq. (2) the integrand is given by:

402

$$403 \quad x_{PD} \sim rV^3 \quad (7)$$

404

405 where  $r$  again arises from the polar integral, and we drop the factor  $\rho C_d$ . Power dissipation  
406 yields a weighting of the radial structure that lies in between dP and IKE (Figure 7). This  
407 behavior arises because  $V^3$  more strongly weights higher wind speeds than  $V^2$ .

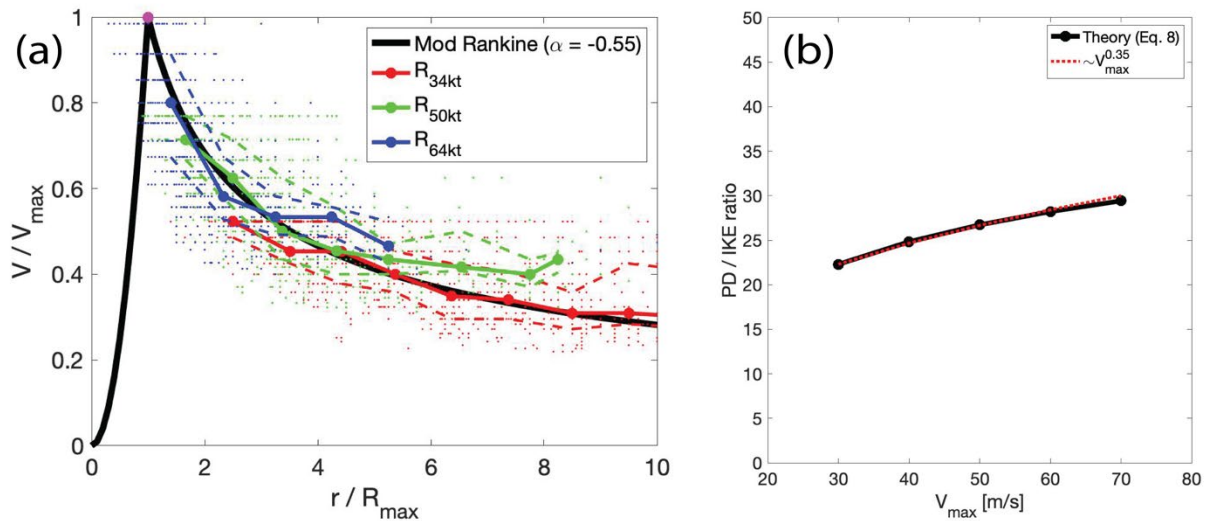
408

409 However, our results are nearly identical when applying our methodology for PD rather than  
 410 IKE. Despite their different weighting structures, variations in PD and IKE correlate very  
 411 strongly with one another ( $r_{\text{rank}} = 0.99$ ; Figure S1). The close relationship between IKE and PD  
 412 arises because the inner wind field is well-approximated by a Modified Rankine vortex (Rappin  
 413 et al. 2013), given by  $\tilde{V} = \tilde{r}^\alpha$ , where  $\tilde{r} = r/R_{\text{max}}$  and  $\tilde{V} = V/V_{\text{max}}$ . The statistics of the  
 414 Extended Best Track wind radii data maps closely onto a Rankine vortex with an exponent  $\alpha =$   
 415  $-0.55$  (Figure 8a). For this wind profile solution, the ratio of PD to IKE between  $R_{\text{max}}$  and  $R_{34kt}$   
 416 can be derived analytically, and may be written as:

$$418 \quad \frac{\text{PD}}{\text{IKE}} \sim \left( \frac{2\alpha+2}{3\alpha+2} \right) V_{\text{max}} \left( \frac{\tilde{V}_{34kt}^{3+\frac{2}{\alpha}} - 1}{\tilde{V}_{34kt}^{2+\frac{2}{\alpha}} - 1} \right) \quad (8)$$

419 where  $\tilde{V}_{34kt} = V_{34kt}/V_{\text{max}}$ ,  $V_{34kt}$  is simply the gale force wind speed, and we have neglected the  
 420 constants in each quantity as described above. This solution neglects winds within the eye  
 421 ( $r < R_{\text{max}}$ ). Eq. 8 shows that, for fixed values of  $\alpha$  and wind speed of the bounding radius ( $V_{34kt}$ ),  
 422 the ratio of PD to IKE depends only on  $V_{\text{max}}$ ; it does not depend on  $R_{\text{max}}$ . Moreover, the  
 423 dependence on  $V_{\text{max}}$  is weak (Figure 8b), following a scaling of approximately  $V_{\text{max}}^{0.35}$ . As a  
 424 result, IKE and PD scale very closely together and are nearly equivalent as predictors for  
 425 historical damage. A more detailed analysis of the relationship between IKE and PD in observed  
 426 storms may be an interesting avenue for future research.

427



428 **Figure 8.** (a) Statistics of Extended Best Track wind radii ( $R_{34kt}$  in blue,  $R_{50kt}$  in green,  $R_{64kt}$   
 429 in red) plotted with radius normalized by the radius of maximum wind speed and wind speed  
 430 normalized by maximum wind speed, for the 2004-2020 southwest Atlantic subset. Median  
 431 (solid) and interquartile range (dashed; 25<sup>th</sup>-75<sup>th</sup> percentile) values of  $(r/R_{\text{max}}, V/V_{\text{max}})$   
 432 calculated within unit bins of  $r/R_{\text{max}}$  (i.e. 1-2, 2-3, etc.); values plotted in bins with at least 10  
 433 datapoints. Modified Rankine profile shown (black) with  $\alpha = -0.55$ . (b) Ratio of PD to IKE for  
 434 the Modified Rankine solution between  $R_{\text{max}}$  and  $R_{34kt}$  (Eq. 8) as a function of  $V_{\text{max}}$  (black),  
 435 with approximate scaling (red) for comparison.

437  
438 Note that technically the weighted-average wind speeds (Table S1) should be recalculated for  
439  $V^3$ , but doing so using a piecewise-linear model of the wind field has a negligible change to this  
440 outcome (not shown).

441  
442 Ultimately there is likely no single “correct” weighting of the radial structure when relating the  
443 wind field to damage potential, as storm hazards (wind, surge, and rainfall) each depend on  
444 different aspects of the wind field in addition to an array of other environmental factors that can  
445 vary from storm to storm. Indeed, our results indicate that IKE and PD are equally useful as  
446 predictors of damage potential despite their different weighting structures. We find that MSLP is  
447 slightly more useful as a damage predictor, suggesting that its weighting structure may be better  
448 suited for representing damage potential or other direct/indirect societal disruptions.  
449 Explanations for why that might be are highly complex, though, and hence we leave this topic  
450 for future work.

## 451 **6 Summary and conclusions**

452 Here we have investigated the relationship between IKE,  $V_{\max}$  and MSLP for both Atlantic basin  
453 hurricanes and for CONUS landfalling hurricanes, specifically from 1988–2020. We find that  
454 IKE has a stronger relationship with MSLP than with  $V_{\max}$ , both for basinwide hurricanes and  
455 CONUS landfalling hurricanes. This finding is likely due to the robust relationship between  
456 storm size and central pressure deficit, as the central pressure is itself an integrated measure of  
457 the wind field. When focusing specifically on well-measured southwest Atlantic hurricanes and  
458 using rank correlations,  $V_{\max}$  explains ~25% of the variance in IKE, while MSLP explains ~40%  
459 of the variance in IKE.

460 Minimum sea level pressure is a better predictor of CONUS landfalling hurricane damage than  
461 IKE and especially  $V_{\max}$ . While all three metrics show strong skillful correlations for hurricanes  
462 making landfall from Texas to Florida, the correlation between  $V_{\max}$  and landfalling hurricane  
463 damage is small and insignificant for hurricanes making landfall from Georgia to Maine. The  
464 degradation in the relationship between  $V_{\max}$  and normalized damage for hurricanes making  
465 landfall along the East Coast of the United States north of Florida is likely due to the growth in  
466 size of hurricanes as they move poleward. Hence, our analysis indicates that the use of MSLP to  
467 categorize hurricane strength would have especially high value for potential landfalls along the  
468 East Coast. Very similar results are obtained when using PD as an integrated wind field quantity  
469 as opposed to IKE because the wind profile is well-approximated by a Modified Rankine profile,  
470 for which the two quantities scale closely with each other.

471  
472 Importantly, an additional benefit of using MSLP to categorize hurricanes is that it is already  
473 routinely measured operationally. Furthermore, it is much simpler to estimate than either the full  
474 hurricane wind field or even  $V_{\max}$  given its relatively noisy nature. In essence, MSLP is a storm-  
475 integrated quantity that can be measured directly (in principle) at a single point at the center of  
476 the storm. In contrast, IKE requires estimating the wind field over a large range of radii along  
477 multiple azimuths. Since MSLP is found to be the best predictor of historical hurricane damage  
478 and is relatively easy to measure, we conclude that MSLP is an ideal metric for categorizing  
479 damage potential for hurricanes. Based on these findings, we advocate for efforts to improve

480 forecasts and interpretation of MSLP as an intensity metric when communicating tropical  
481 cyclone societal risk to the general public.

## 482 **Acknowledgments**

483 P. Klotzbach would like to acknowledge a grant from the G. Unger Vetlesen Foundation. D.  
484 Chavas acknowledges NSF Grants 1826161 and 1945113. M. Bell was supported by Office of  
485 Naval Research Grant N000142012069. C. Schreck was supported by NOAA through the  
486 Cooperative Institute for Satellite Earth System Studies under Cooperative Agreement  
487 NA19NES4320002. E. Gibney's research at the National Hurricane Center is supported by  
488 NOAA's Science Collaboration Program and administered by UCAR's Cooperative Programs for  
489 the Advancement of Earth System Science (CPAESS) under award NA21OAR4310383.

## 490 **Data Availability Statement**

491 All data used in this study are publicly available at the following locations:

492

493 *Extended Best Track:*

494

495 [https://rammb2.cira.colostate.edu/research/tropical-cyclones/tc\\_extended\\_best\\_track\\_dataset/](https://rammb2.cira.colostate.edu/research/tropical-cyclones/tc_extended_best_track_dataset/)

496

497 *Continental US Hurricane Landfalls:*

498

499 [https://www.aoml.noaa.gov/hrd/hurdat/UShurrs\\_detailed.html](https://www.aoml.noaa.gov/hrd/hurdat/UShurrs_detailed.html)

500

501 *Normalized Continental US Hurricane Damage (1988–2017):*

502

503 [https://static-content.springer.com/esm/art%3A10.1038%2Fs41893-018-0165-  
504 2/MediaObjects/41893\\_2018\\_165\\_MOESM2\\_ESM.xlsx](https://static-content.springer.com/esm/art%3A10.1038%2Fs41893-018-0165-2/MediaObjects/41893_2018_165_MOESM2_ESM.xlsx)

505

506 *Normalized Continental US Hurricane Damage (2018–2020):*

507

508 <https://www.nhc.noaa.gov/data/tcr/>

## 509 **References**

510 Bister, M. & Emanuel, K.A. (1998). Dissipative heating and hurricane intensity. *Meteorology  
511 and Atmospheric Physics*, 65(3), 233–240. <https://doi.org/10.1007/BF01030791>

512 Buchanan, S., Misra, V., & Bhardwaj, A. (2018). Integrated kinetic energy of Atlantic tropical  
513 cyclones in a global ocean surface wind analysis. *International Journal of Climatology*, 38(6),  
514 2651–2661. <https://doi.org/10.1002/joc.5450>.

515 Chavas D .R., & Knaff, J. A. (2022). A simple model for predicting the tropical cyclone radius of  
516 maximum wind from outer size. *Weather and Forecasting*, Early Online Release.

517 <https://doi.org/10.1175/WAF-D-21-0103.1>

518 Chavas, D. R., Lin, N., Dong, W., & Lin, Y. (2016). Observed tropical cyclone size revisited.

519 *Journal of Climate*, 29(8), 2923–2939. <https://doi.org/10.1175/JCLI-D-15-0731.1>

- 520 Chavas, D. R., Reed, K. A., & Knaff, J. A. (2017). Physical understanding of the tropical cyclone  
521 wind-pressure relationship. *Nature Communications*, 8, 1360. [https://doi.org/10.1038/s41467-](https://doi.org/10.1038/s41467-017-01546-9)  
522 [017-01546-9](https://doi.org/10.1038/s41467-017-01546-9)
- 523 Chavas D. R., Reed, K. A., & Knaff, J. A. (2018). Conference notebook: Physical understanding  
524 of the tropical cyclone wind-pressure relationship. *Bulletin of the American Meteorological*  
525 *Society*, 99(12), 2449.  
526 [https://web.ics.purdue.edu/~dchavas/download/ChavasReedKnaff2018BAMS\\_TCWindPressure](https://web.ics.purdue.edu/~dchavas/download/ChavasReedKnaff2018BAMS_TCWindPressure)  
527 [ConferenceNotebookSandyExample.pdf](https://web.ics.purdue.edu/~dchavas/download/ChavasReedKnaff2018BAMS_TCWindPressure)
- 528 Demuth, J. L., DeMaria, M., & Knaff, J. A. (2006). Improvement of advanced microwave  
529 sounding unit tropical cyclone intensity and size estimation algorithms. *Journal of Applied*  
530 *Meteorology and Climatology*, 45(11), 1573–1581. <https://doi.org/10.1175/JAM2429.1>
- 531 Efron, B., (1979). Bootstrap methods: Another look at the jackknife. *The Annals of Statistics*,  
532 7(1), 1–26. <https://doi.org/10.1214/aos/1176344552>
- 533 Emanuel, K.A., (1999). The power of a hurricane: An example of reckless driving on the  
534 information superhighway. *WEATHER-LONDON*, 54, 107-108.
- 535 Grinsted, A., Ditlevsen, P., & Christensen, J. H. (2019). Normalized US hurricane damage  
536 estimates using area of total destruction, 1900–2018. *Proceedings of the National Academy of*  
537 *Sciences*, 116(48), 23942–23946. <https://doi.org/10.1073/pnas.1912277116>
- 538 Halverson, J. B., & Rabenhorst, T. (2013). Hurricane Sandy: The science and impacts of a  
539 superstorm. *Weatherwise*, 66(2), 14–23. <https://doi.org/10.1080/00431672.2013.762838>
- 540 Hesterberg, T. S., Monaghan, S., Moore, D. S., Clipson, A., Epstein, R. (2003). Bootstrap  
541 methods and permutation tests. Companion chapter 18 to *The Practice of Business Statistics*. W.  
542 H. Freeman and Company, New York, 85 pp.  
543 <https://statweb.stanford.edu/~tibs/stat315a/Supplements/bootstrap.pdf>
- 544 Irish, J. L., Resio, D. T., & Ratcliff, J. J. (2008). The influence of storm size on hurricane surge.  
545 *Journal of Physical Oceanography*, 38(9), 2003–2013. <https://doi.org/10.1175/2008JPO3727.1>
- 546 Klotzbach, P. J., Bell, M. M., Bowen, S. G., Gibney, E. J., Knapp, K. R., & Schreck, C. J., III.  
547 (2020). Surface pressure a more skillful predictor of normalized hurricane damage than  
548 maximum sustained wind, *Bulletin of the American Meteorological Society*, 101(6), E830–E846.  
549 <https://doi.org/10.1175/BAMS-D-19-0062.1>
- 550 Klotzbach, P. J., Bowen, S. G., Pielke Jr., R., & Bell, M. M. (2018). Continental United States  
551 landfall frequency and associated damage: Observations and future risks. *Bulletin of the*  
552 *American Meteorological Society*, 99(7), 1359–1376. [https://doi.org/10.1175/BAMS-D-17-](https://doi.org/10.1175/BAMS-D-17-0184.1)  
553 [0184.1](https://doi.org/10.1175/BAMS-D-17-0184.1)
- 554 Knaff, J. A., Longmore, S. P., & Molenaar, D. A. (2014). An objective satellite-based tropical  
555 cyclone size climatology. *Journal of Climate*, 27(1), 455–476. [https://doi.org/10.1175/JCLI-D-](https://doi.org/10.1175/JCLI-D-15-0610.1)  
556 [15-0610.1](https://doi.org/10.1175/JCLI-D-15-0610.1)

- 557 Knaff, J. A., & Zehr, R. M. (2007). Reexamination of tropical cyclone wind-pressure  
558 relationships. *Weather and Forecasting*, 22(1), 71–88. <https://doi.org/10.1175/WAF965.1>
- 559 Kozar, M. E., & Misra, V. (2014). Statistical prediction of integrated kinetic energy in North  
560 Atlantic tropical cyclones. *Monthly Weather Review*, 142(12), 4646–4657.  
561 <https://doi.org/10.1175/MWR-D-14-00117.1>.
- 562 Landsea, C. W., & Franklin, J. L. (2013). Atlantic hurricane database uncertainty and  
563 presentation of a new database format. *Monthly Weather Review*, 141(10), 3576–3592.  
564 <https://doi.org/10.1175/MWR-D-12-00254.1>
- 565 Lee, I. A., & Preacher, K. J. (2013). Calculation for the test of the difference between two  
566 dependent correlations with one variable in common [Computer software]. Available from  
567 <http://quantpsy.org>.
- 568 Lonfat, M., Rogers, R., Marchok, T., & Marks, F. D. (2007). A parametric model for predicting  
569 hurricane rainfall. *Monthly Weather Review*, 135(9), 3086–3097.  
570 <https://doi.org/10.1175/MWR3433.1>.
- 571 Maclay, K. S., DeMaria, M., Vonder Haar, T. H. (2008). Tropical cyclone inner-core kinetic  
572 energy evolution. *Monthly Weather Review*, 136(12), 4882–4898,  
573 <https://doi.org/10.1175/2008MWR2268.1>.
- 574 Mendelsohn, R., Emanuel, K., Chonabayashi, S., & Bakkensen, L. (2012). The impact of climate  
575 change on global tropical cyclone damage. *Nature Climate Change*, 2, 205–209,  
576 <https://doi.org/10.1038/nclimate1357>.
- 577 Misra, V., DiNapoli, S., & Powell, M. (2013). The track integrated kinetic energy of Atlantic  
578 tropical cyclones. *Monthly Weather Review*, 141(7), 2383–2389, [https://doi.org/10.1175/MWR-](https://doi.org/10.1175/MWR-D-12-00349.1)  
579 [D-12-00349.1](https://doi.org/10.1175/MWR-D-12-00349.1).
- 580 Powell, M. D., & Reinhold, T. A. (2007). Tropical cyclone destructive potential by integrated  
581 kinetic energy. *Bulletin of the American Meteorological Society*, 88(4), 513–526,  
582 <https://doi.org/10.1175/BAMS-88-4-513>.
- 583 Rappin, E. D., Nolan, D. S. & Majumdar, S. J. (2013). A highly configurable vortex initialization  
584 method for tropical cyclones. *Monthly Weather Review*, 141(10), 3556–3575.  
585 <https://doi.org/10.1175/MWR-D-12-00266.1>.
- 586 Schott, T., & Coauthors. (2012): The Saffir–Simpson hurricane wind scale. National Hurricane  
587 Center, <http://www.nhc.noaa.gov/pdf/sshws.pdf>.
- 588 Simpson, R. H. (1974). The hurricane disaster potential scale. *Weatherwise*, 27(4), 169, 186,  
589 <https://doi.org/10.1080/00431672.1974.9931702>.
- 590 Weinkle, J., Landsea, C., Collins, D., Masulin, R., Crompton, R. P., Klotzbach, P. J., & Pielke Jr.,  
591 R. P. (2018). Normalized hurricane damage in the continental United States 1900–2017. *Nature*  
592 *Sustainability*, 1(12), 808–813. <https://doi.org/10.1038/s41893-018-0165-2>